Journal Pre-proof

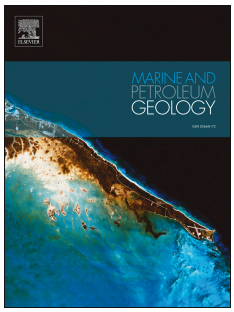

Sedimentological and ichnological analyses of the continental to marginal-marine Centenario Formation (Cretaceous), Neuquén Basin, Argentina: Reservoir implications

Alina Shchepetkina, Juan José Ponce, Noelia Beatriz Carmona, M. Gabriela Mángano, Luis A. Buatois, Soledad Ribas, Marcela Celeste Villar Benvenuto

PII: S0264-8172(20)30254-3

DOI: https://doi.org/10.1016/j.marpetgeo.2020.104471

Reference: JMPG 104471

To appear in: *Marine and Petroleum Geology*

Received Date: 28 March 2020

Revised Date: 14 May 2020

Accepted Date: 15 May 2020

Please cite this article as: Shchepetkina, A., Ponce, Juan.José., Carmona, N.B., Mángano, M.G., Buatois, L.A., Ribas, S., Villar Benvenuto, M.C., Sedimentological and ichnological analyses of the continental to marginal-marine Centenario Formation (Cretaceous), Neuquén Basin, Argentina: Reservoir implications, *Marine and Petroleum Geology* (2020), doi: https://doi.org/10.1016/j.marpetgeo.2020.104471.

CRediT author statement

Shchepetkina A.: Conceptualization, Methodology, Validation, Formal analysis, Investigation, Writing - Original Draft, Writing - Review & Editing, Visualization, Project administration

Ponce J.J.: Conceptualization, Methodology, Supervision, Funding acquisition

Carmona N.B.: Conceptualization, Methodology, Supervision, Funding acquisition

Mángano M.G.: Validation, Writing - Review & Editing, Supervision

Buatois L.A.: Validation, Writing - Review & Editing, Supervision

Ribas S.: Conceptualization, Resources, Investigation

Villar Benvenuto M.C.: Conceptualization, Resources, Investigation

Sedimentological and ichnological analyses of the continental to marginal-marine Centenario Formation (Cretaceous), Neuquén Basin, Argentina: Reservoir implications

Alina Shchepetkina [a,b,*], Juan José Ponce [a], Noelia Beatriz Carmona [a], M. Gabriela Mángano [b], Luis A. Buatois [b], Soledad Ribas [c], Marcela Celeste Villar Benvenuto [c]

[a] Instituto de Investigación en Paleobiología y Geología – Universidad Nacional de Río Negro, General Roca, Río Negro, Argentina 8332

[b] Department of Geological Sciences, University of Saskatchewan, Saskatoon, SK, Canada S7N 5E2

[c] YPF, Talero 360, Neuquén, Neuquén, Argentina 8300

alinashch@gmail.com

ABSTRACT

The upper Valanginian – lower Aptian Centenario Formation is a significant producer of oil and gas in the Neuquén Basin, western Argentina. This formation is located exclusively in the subsurface of the eastern and northeastern Neuquén Basin, and is 450-1000 m thick. The Centenario Formation laterally interfingers with the Agrio Formation. Previous studies addressing the paleogeographic history of the Centenario Formation are scarce, and a comprehensive geological model has yet to be put forward.

The current study scrutinizes the Centenario Formation, especially its lower member, within the northeastern Neuquén Basin. The study area includes the Cerro Hamaca Oeste, Señal Cerro Bayo, and Volcán Auca Mahuida oilfields operated by Yacimientos Petrolíferos Fiscales (YPF). Sedimentological and ichnological core data, geophysical well logs, and petrographic thin sections have been utilized to construct a geological model. Eleven sedimentary facies and three facies associations have been identified from the core dataset, providing insights into the paleoenvironmental settings and their stresses on infaunal colonization. Basin-margin deposits from the northeastern part of the study region were formed in continental environments, comprising ephemeral fluvial channel complexes and floodplains, and are ichnologically represented by rare *Skolithos* and common rhizoliths. The central part of the study area is interpreted as recording deposition in ephemeral lakes, river-dominated lake deltas, and coastal lagoons and sabkhas, and is represented by a combination of stressed expressions of both the *Skolithos* and *Scoyenia* Ichnofacies. River-dominated, storm-influenced delta deposits are located towards the southwestern limit of the study area, and are ichnologically represented by the *Skolithos* and depauperate *Cruziana* Ichnofacies. Deltaic deposits gradually transition into the

basinal facies of the Agrio Formation to the west. Overall sedimentologic characteristics suggest semi-arid to arid climatic conditions during deposition.

Keywords: Paleoenvironmental reconstruction; Trace fossils; Fluvial; Lakes; Deltas; Embayment; Petroleum geology

1. INTRODUCTION

A total of 800 million m^3 of oil-equivalent comprising 60% gas are contained within the Jurassic and Cretaceous succession of the Neuquén Basin, making it an important petroleum producer (Hogg, 1993). Medium-weight oil (28-35 API) and wet gas are commonly extracted from the Centenario Formation. The Valanginian to lower Aptian (Lower Cretaceous) Centenario Formation is located entirely in the subsurface of eastern, northeastern and southeastern Neuquén Basin and is 450-1000 m thick. Originally, the unit was defined by Digregorio (1972), and is represented by conglomeratic sandstone and shale of continental and marginal-marine origin. The Centenario Formation laterally interfingers with the Agrio Formation to the west.

This study presents a detailed sedimentological and ichnological characterization of the Centenario Formation. From a sedimentological perspective, the main objectives of this study are to: 1) document different sedimentary facies and facies associations and 2) suggest an integrated geological model that adequately explains the distribution of sedimentary facies, allowing for prediction of the main reservoir trends within the oilfields. From an ichnological perspective, the study aims to establish the ichnological assemblages present and to refine paleoenvironmental interpretations. This aspect of the study is critical as stressful environmental conditions play a major role in controlling the response by the benthos and their interactions with the substrate, imparting detectable signals in the trace-fossil record. Although trace fossils have been widely used to detect departures from normal marine salinity (e.g., Howard and Frey, 1973, 1975; Dörjes and Howard, 1975; Pemberton and Wightman, 1992; MacEachern and Pemberton, 1994; Gingras et al., 1999; Buatois et al., 2005; MacEachern and Gingras, 2008; Gingras and MacEachern, 2012; Shchepetkina et al., 2016; Solórzano et al., 2017), the number of studies documenting ichnologic trends along salinity gradients, from freshwater to brackish water and normal-marine salinity

conditions within single stratigraphic units are still relatively scarce (e.g., Mángano and Buatois, 2004; Solórzano et al., 2017). A regional-scale paleoenvironmental reconstruction of the continental to marginal-marine Centenario Formation further enhances our understanding of trace-fossil assemblages in a back-arc basin setting and allows evaluation of how lateral facies transitions affect the reservoir continuity and quality.

2. GEOLOGICAL SETTING

The Lower Cretaceous Centenario Formation is located in the Neuquén Basin, which formed during the subduction of the southern Nazca Plate under the South American Plate (Hogg, 1993). The basin has a triangular shape (Fig. 1), and is subdivided into two main zones: the Andes region and the Neuquén Embayment region; the study area lies within the confines of the petroliferous embayment region. The basin is limited on its northeastern and southern margins by wide cratonic areas of the Sierra Pintada Massif and the North Patagonian Massif, respectively (Fig. 1b). On the western margin, the basin was bounded by the Andean magmatic arc until the end of the Early Cretaceous (Howell et al., 2005).

The basin records more than 7,000 m of strata deposited from the Late Triassic to the Cenozoic, consisting of conglomerate, sandstone, siltstone, shale, carbonate, and evaporite that were deposited in a multitude of depositional settings (Vergani et al., 1995; Howell et al., 2005). Deposition occurred during three phases: the Upper Triassic intraplate rifting, the Lower-Middle Jurassic back-arc basin development (including the formation of interest, Fig. 2), and the Upper Cretaceous – Cenozoic foreland basin regime (Vergani et al., 1995; Howell et al., 2005; Schwarz and Howell, 2005).

The Centenario Formation consists of reddish clastic deposits widely distributed on the Neuquén Basin platform (Digregorio, 1972), and represents an exclusively subsurface, marginal-marine to continental equivalent of the shale-dominated Agrio Formation (Mendiberri, 1984; Spalletti and Veiga, 2011). The formation is informally subdivided into the lower and upper members (Fig. 2b) (Cabaleiro, 2002; Cabaleiro et al., 2002; Casadío and Montagna, 2015; Cevallos et al., 2008; Soraci et al., 2010) with previous paleoenvironmental interpretations being quite variable (Table 1).

The lower Centenario member is about 350 m thick and spans the upper Valanginian to lower Hauterivian (Fig. 2b) (Cabaleiro, 2002; Cabaleiro et al., 2002). The onset of deposition began with a marine transgression (TST) and continued during a highstand systems tract (HST) (Rebasa et al., 1992; Vottero and Cafferata, 1992; Cabaleiro et al., 2002; Iñigo et al., 2019). A relatively shallow sea covered the Neuquén Embayment at that time (Fig. 1b), and strata of the HST are suggested to be deposited in littoral, deltaic, estuarine, and distal fluvial paleoenvironments (Cabaleiro et al., 2002; Cabaleiro, 2002; Cevallos et al., 2008; Casadío and Montagna, 2015; Iñigo et al., 2019). The top of the lower Centenario member is marked by an important sea-level fall that generated a sequence boundary (Cabaleiro et al., 2002; Cevallos et al., 2008; Iñigo et al., 2019). This Intra-Hauterivian unconformity (Fig. 2b) developed when the connection with the paleo-Pacific Ocean was restricted, which caused initiation of continental deposition, including the development of ephemeral rivers, aeolian sand seas, playa lakes, and sabkhas (Cevallos et al., 2008; Casadío and Montagna, 2015). The upper Centenario member is about 240 m thick. Its deposition started with another transgressive interval (TST), which is overlain by a progradational clastic system (HST), mainly representing the fluvial system (Cabaleiro et al., 2002; Casadío and Montagna, 2015; Iñigo et al., 2019). The distinction between the lower and upper

Centenario members becomes increasingly difficult towards the eastern limit of the Neuquén Basin due to their lithological similarity.

3. STUDY AREA

The study area includes three oilfields: Cerro Hamaca Oeste (CHO), Señal Cerro Bayo (SCB), and Volcán Auca Mahuida (VAM) (Figs. 3-4). These oilfields are located on the platformal, shallow part of the Neuquén Basin (Fig. 3a) (Delpino et al., 2014), where the Centenario Formation serves primarily as a reservoir. The underlying Vaca Muerta and Quintuco formations form the source rocks, and a variety of shale, diagenetically altered rocks, and dikes form the cap rock within the Centenario Formation (Delpino et al., 2014). The predominant trap type is structural, as represented by a regional northwest-southeast oriented anticline affected by igneous activity and smaller dome structures. The regional anticline is likely related to the basement structures (Iñigo et al., 2019). Stratigraphic traps occur due to a change in facies type or diagenetic changes in rock composition (Cevallos and Rivero, 2009; Delpino et al., 2014). Migration pathways are typically attributed to the normal faults that cross-cut the sedimentary package.

The CHO oilfield is situated in the northwestern part of the study region (Figs. 3b-4). It sits on the northwest-southeast oriented anticlinal structure (Soraci et al., 2010). Only the upper Centenario member has undergone production with 24 drilled wells reported (Soraci et al., 2010). Two cores from the upper Centenario member (CHO.e-2 and CHO.e-4) have been analyzed in the current study. The SCB oilfield covers the northeastern part of the Auca Mahuida volcano (Figs. 3b-4) and is situated atop the anticline striking in the northwest-southeast direction (Cabaleiro, 2002). Both Centenario members are productive in the SCB oilfield (Soraci et al., 2010), with a total of 113 drilled wells. From this oilfield, nine cores from the lower Centenario member have

been analyzed in this study (SCB-8, 9, 10, 11, 27, 51, 52, 59, 102). The VAM oilfield produces oil, and to a lesser extent gas (Schwarz et al., 2008), and occupies the northern part of the Auca Mahuida volcano (Figs. 3b-4). The oilfield is defined by a large, complex anticline oriented north-southwest and cross-cut by numerous faults (Vela et al., 2006; Schwarz and Veiga, 2007; Delpino et el., 2014). The lower Centenario member has been productive in the VAM oilfield with 89 drilled wells. One core (VAM-80) has been analyzed in the current study.

In regards to probable sediment provenance, the study area is bordered to the northeast and east by the Sierra Pintada Massif (Fig. 5). In the area closest to the studied oilfields, the Sierra Pintada consists of the Las Matras and Chadileuvú blocks (Fig. 5) (Cingolani and Heredia, 2001). The Las Matras pluton is characterized by magmatic arc facies (Sato et al., 2000), and consists of late Proterozoic tonalite and trondhjemite, intruded Paleozoic granite, upper Cambrian to Lower Ordovician limestone and marble, upper Carboniferous quartzite, and Permo-Triassic volcanic rocks (Sato et al., 2000; Llambías et al., 2003). The Chadileuvú block is located approximately 150 km south-east from the Las Matras block, and consists of the lower Paleozoic granodiorite and monzogranite, Ordovician metamorphic rocks, Permian sedimentary rocks, and Permo-Triassic volcanic rocks (Sato et al., 2000; Llambías et al., 2003). Similarly, Iñigo et al. (2019) proposed a local eastward and northeastward sediment supply for the Centenario Formation within the northeastern border of the Neuquén Basin.

4. DATABASE AND METHODOLOGY

The study is based on the following data: 1) 12 cores (~261 m) from the CHO, SCB, and VAM oilfields (Figs. 4-6); 2) 104 petrographic thin sections; and 3) a previously created Petrel project

(property of YPF) with well locations, basic geophysical well logs (e.g., GR, SP), formation tops, and lease contours.

The applied methodology included: 1) compilation of the aforementioned data; 2) detailed sedimentological and ichnological descriptions of cores; 3) description of petrographic thin sections; 4) integration of datasets (i.e., geophysical well logs, sedimentological and ichnological data, photos of box cores); 5) definition and interpretation of facies and facies associations; 6) correlation of facies associations using geophysical well logs; and 7) proposal of a conceptual paleoenvironmental model based on stratigraphic analysis, facies analysis, and literature review.

Sedimentological and ichnological descriptions were undertaken using the cores located in the Avellaneda Core Research Facility (Buenos Aires) in August and November 2017. The core was manually logged and later re-drawn using Adobe Illustrator©. Data collected included bed thicknesses, bed and facies contacts, physical sedimentary structures, grain size, lithologic accessories, trace fossils identified at the ichnogenus level, and bioturbation index (Reineck, 1963; Taylor and Goldring, 1993). Core boxes were photographed in indoor artificial light with a focus on diagnostic primary sedimentary and ichnological features.

For the preparation of thin sections, samples were washed with toluene to eliminate the presence of hydrocarbons. Later, the samples were impregnated with Epoxy Blue resin to highlight pore distributions. Some thin sections were also saturated with Alizarin Red-S (red dye) to differentiate calcite from dolomite. Grain sizes were determined based on the Udden-Wentworth scale. Description of petrographic thin sections was done using the Nikon ECLIPSE E200 POL optical microscope at the Instituto de Investigación en Paleobiología y Geología (General Roca, Argentina) and Avellaneda Core Research Facility (Buenos Aires, Argentina). Microscopic photos were obtained using Zeiss Axio Imager M2m microscope with an attached

camera Axiocam 506 Color at the Microscopy-Spectroscopy Laboratory, YPF-Tecnología (La Plata, Argentina).

5. SEDIMENTARY FACIES AND DEPOSITIONAL MODEL

Eleven distinct facies were identified in cores, F1-F11 (Figs. 7-9). Detailed facies descriptions and paleodepositional interpretations are provided in Table 2. The subdivision of facies was based on the predominant lithology, grain size, bed contacts, and physical and biogenic sedimentary structures.

Three main facies associations identified in the study area (Table 3, Figs. 10-11) record continental to shallow-marine depositional environments (Fig. 12). These facies associations stack vertically and show the evolution of the landscape through time. Their identification was based on the combination of related individual facies identified through core analysis. The facies associations are FA1 – continental (fluvio-lacustrine), FA2 – continental to marginal-marine (lake, coastal lagoon, delta plain), and FA3 – shallow-marine (deltaic).

FA1 consists of F1-F3, and records continental deposition. It is present in the northern and northeastern parts of the study area. This association occurs in the lower Centenario member in the eastern part of the SCB oilfield (Fig. 10) and in the upper Centenario member in the CHO oilfield (Fig. 10). It represents an aggradational depositional pattern with an increase in sandbody thickness and lateral distribution towards the northeast. In the lower Centenario member, the change from the purely continental (FA1) to the predominantly marginal-marine (FA2) regime is detected in the SCB area, somewhere between wells SCB-51 and SCB-27 (Fig. 10). Data on the upper Centenario member is extremely scarce, and direct observations only exist within two short,

cored wells in the CHO area (Fig. 10). Based on those data points and on regional information, it is suggested that the upper Centenario member mostly records continental environments.

FA2 consists of F4-F8, and represents sedimentation in continental to marginal-marine environments. FA2 has been recognized in the lower Centenario member in the SCB and VAM areas (Figs. 10-11). The succession shows a general progradational and aggradational depositional pattern. Its thickness and areal distribution increase in the southwest direction towards the center of the Neuquén Basin. Its areal extent further to the northeast and southwest is unknown due to the absence of data. It is proposed that FA2 grades into FA1 towards the northeast and into FA3 (or its open-marine equivalents, i.e. the Agrio Formation) to the southwest.

FA3 consists of F9-F11, and records deposition in shallow-marine (deltaic) settings. This association occurs in the basal interval of the lower Centenario member in the VAM and SCB areas (Figs. 10-11). FA3 likely possesses a progradational character with delta lobes extending and thickening to the southwest towards the center of the Neuquén Basin (Figs. 10-12).

6. ICHNOLOGICAL EVIDENCE AND EVALUATION OF PALEOENVIRONMENTAL STRESS FACTORS

Integration of ichnological and sedimentological dataset allows for more precise determination of the paleodepositional settings and possible identification of physico-chemical stresses present during deposition in individual facies and facies associations.

Continental deposition is represented by FA1, characterized by complexes of ephemeral freshwater fluvial channels, crevasse splays, surrounding floodplains, and paleosols. Although each of these depositional environments tends to be characterized by a different trace-fossil assemblage (Melchor et al., 2012), it is generally accepted that the ichnofacies recognized in

continental deposits include, among others, the *Scoyenia* and *Skolithos* Ichnofacies (Buatois and Mángano, 2007). In the Centenario Formation, belts of migrating, ephemeral freshwater fluvial channels and associated crevasse splays (F1-F2) are mostly barren of trace fossils with only rare occurrences of small, vertical shafts of monospecific suites of *Skolithos* in discrete layers (BI 0-1), representing a continental occurrence of the *Skolithos* Ichnofacies (Buatois and Mángano, 2004, 2007). General lack of bioturbation is explained by highly stressful physicochemical conditions, such as periodically high sedimentation rates, generally high and fluctuating temperatures, sediment desiccation, and prolonged sediment exposure with rapid precipitation of infilling cements, all typical of an arid climate. Paleosols (F3) of FA1 bound the ephemeral channel complexes, and host abundant, penetrative and relatively straight rootlets, which indicate a low water table and sporadically available water (Cohen, 1982; Bockelie, 1994; Retallack, 2001). Vegetation in semi-arid climates is generally established in areas of abundant surficial and subterraneous water (e.g., floodplains of non-perennial channels, streams, crevasse splays, lakes), and is exceptionally sparse elsewhere (Cohen, 1982).

Continental to marginal-marine environments are represented by FA2 with an array of facies interpreted as ephemeral lakes and their margins, various upper delta-plain environments, distributary channels and mouth bars of river-dominated deltas debouching into lakes and lagoons, and shallow coastal lagoons/sabkhas. The bioturbation signature in these environments is more pronounced and characterized by predominantly low to moderate ichnodiversity, sporadic trace-fossil distribution, and bioturbation intensity ranging from absent to moderate (BI 0-4). Shallow-water ephemeral lakes and their margins (F4) are typified by the *Scoyenia* Ichnofacies (*sensu* Buatois and Mángano, 1995, 1998; Scott et al., 2012), which indicates moist to wet, muddy to sandy substrates at low energy sites with conditions changing between fully

aquatic and subaerial, and periodically stressful physicochemical conditions. Stressors influencing the infauna likely include temperature variations, prolonged subaerial exposure (manifested by common secondary cements, mudstone rip-up clasts, brecciated microbialites), rapid sedimentation rates, and variable salinity levels (evidenced by syneresis cracks) with seasonal occurrence of hypersaline conditions (denoted by local microbial mats). Upper delta plain environments, especially crevasse channels/splays (F5), demonstrate colonization by vegetation with the formation of rhizoliths and vermiform organisms/insects producing *Taenidium* (see fig. 8.17d in Buatois and Mángano, 2011). Such rootlets at the top of the crevasse channel/splay deposits and appearance of *Taenidium* likely represent temporary hiatuses in deposition. A similar ichnological signature has been documented elsewhere (e.g., Martinius et al., 2012; Gugliotta et al., 2015; Diez-Canseco et al., 2015; Solórzano et al., 2017; Rodríguez et al., 2018), including classic examples from the Mississippi River delta (Arndorfer, 1973; Cahoon et al., 2011). The trace-fossil association represents a combination of the *Skolithos* and *Scoyenia* Ichnofacies (*sensu* Buatois and Mángano, 1995, 1998), typical for fluvio-lacustrine environments (Buatois and Mángano, 2004). The *Skolithos* Ichnofacies indicates high-energy conditions (Buatois and Mángano, 1998) common for crevasse channels and splays. The *Scoyenia* Ichnofacies points to moist, non-marine, and shallow aquatic substrates, which are periodically exposed to air (Frey et al., 1984; Buatois and Mángano, 2002). The absence of striated trace fossils, typical of the firmground suite of the *Scoyenia* Ichnofacies implies a soft substrate (Savrda et al., 2000; Buatois and Mángano, 2004). Terminal distributary channels and mouth bars of a river-dominated delta (F6) debouching into the shallow, freshwater and periodically brackish-water receiving body contain a stressed trace-fossil assemblage dominated by indistinct or cryptic bioturbation, with a few discrete trace fossils (e.g., *Palaeophycus, Lockeia).* Presence of resting traces (*Lockeia*) indicates the activity of

suspension- or deposit-feeding bivalves, and suggests abundant detritus either in the water column or on the sediment under moderate-energy conditions (Mángano et al., 1998). Common cryptic bioturbation is caused by meiofauna or small infauna (e.g., 0.1-1 mm wide, juvenile amphipods, nematodes) and is typical for marginal-marine and, more rarely, continental deposits, where animals cause active sediment disruption through grain ingestion (Howard and Frey, 1975; Bromley, 1996; Gingras et al., 2008; Gunn et al., 2008; Shchepetkina et al., 2016). Selective-feeding strategy of meiobenthos similarly points to the abundance of organic material distributed in the sediments. Shallow-water bodies and surrounding mudflats (F7) are typified by a mixture of non-marine occurrences of the *Skolithos* and *Scoyenia* Ichnofacies (Buatois and Mángano, 2011), indicating moist to wet, muddy to sandy substrates, conditions changing between fully aquatic and subaerial, and periodically stressful physicochemical conditions that likely included unstable soupy substrates (indicated by abundant soft-sediment deformation structures, syn-depositional microfaults, and floating grains), intermittently rapid sedimentation rates, variable salinity levels (revealed by syneresis cracks), and temperature variations, among others stressors. Finally, coastal lagoon/sabkha depositional sites (F8) represent an example of the depauperate *Cruziana* Ichnofacies. Although this ichnofacies is typical of stressful, brackish-water settings (e.g., Gingras et al., 1999), depauperate expressions of this ichnofacies are also known from harsh, hypersaline marine settings (e.g., de Gibert and Ekdale, 1999, 2002; Jaglarz and Uchman, 2010; Mercedes-Martin and Buatois, 2020). Trophic generalists dominate this low-diversity association, and indicate highly stressed environmental conditions. Environmental stressors likely include variable water salinity caused by periodically hypersaline conditions, continental freshwater groundwater recharge, and periodic influx of marine water (Zonneveld et al., 2001).

The Centenario river-dominated, storm-influenced delta encompasses proximal (e.g., distributary channels, mouth bars, delta front) and more distal (e.g., prodelta) environments, and is expressed in FA3. The ichnofossil suites are characterized by increased ichnodiversity in comparison with FA1-FA2 and highly variable bioturbation intensity (BI 0-6), indicating fluctuating salinities and alternation of episodic and background sedimentation. Small size of some ichnotaxa (e.g., *Ophiomorpha*) is consistent with reduced salinity (Pemberton and Wightman, 1992). Proximal parts of the delta (F9) show low trace-fossil diversity, opportunistic behaviors (i.e., predominance of simple trace-fossil morphologies with poorly specialized feeding strategies, such as *Skolithos*), and the predominant *Skolithos* Ichnofacies with elements of the depauperate *Cruziana* Ichnofacies. These suites indicate a number of physicochemical stresses, including: 1) changes in water salinity due to fluvial input, 2) increase in water turbidity and phytodetrital content during the freshets, 3) periods with extremely high sedimentation rates during high river discharge and/or storms (e.g., indicated by fugichnia), and 4) mobile sandy substrates due to wave/storm action. Notably, actively migrating bedforms combined with high sedimentation rates may restrict abundance and type of animals inhabiting such substrates, where only deep burrowers (e.g., decapod crustaceans forming *Ophiomorpha*) are able to survive (Pollard et al., 1993; Dashtgard, 2011; Dashtgard and Gingras, 2012). Additional evidence supporting a deltaic interpretation comes from the presence of abundant, rosette-shaped *Haentzschelinia* that tends to occur in shallow-water, nutrient-rich siliciclastic environments with high sedimentation rates (Fürsich and Bromley, 1985; Agirrezabala and De Gibert, 2004). The presence of suspension-feeding burrows, which is rare in deltaic settings affected by elevated levels of water turbidity (MacEachern et al., 2005), may suggest winnowing of fine-grained material by waves, further arguing against a purely river-dominated delta and pointing to wave influence instead. Delta front

(F10) deposits demonstrate an increased storm influence, as indicated by the presence of "lam-scram" intervals. The laminated portion consists of erosionally amalgamated hummocky (HCS) and swaley (SCS) cross-stratified sandstone, recording high-energy combined flows during repeated storm events. Associated escape structures (fugichnia) are formed when organisms try to reach a new sediment-water interface during a storm, whereas the overprinting trace-fossil suite (e.g., cryptic bioturbation, *Ophiomorpha*, *Palaeophycus*, *Skolithos, Diplocraterion, Haentzschelinia)* represents colonization of the storm deposits by opportunistic trace makers. These storm-dominated intervals are punctuated by periods of quiescence, characterized by more intense degree of bioturbation and (scrambled intervals) with moderately diverse suite (e.g., *Ophiomorpha*, *Skolithos, Lockeia*, *?Diplocraterion, Bergaueria, Thalassinoides, Haentzschelinia, Planolites*, *Teichichnus*), recording the re-establishment of an equilibrium population of trace makers (Frey, 1990; Frey and Goldring, 1992; Pemberton and MacEachern, 1997; Buatois et al., 2015). Further seaward, in the prodelta (F11), the presence of typical marine ichnogenera (e.g., *Asterosoma, Chondrites*, *Phycosiphon)* indicate slower, continuous rates of deposition in near-normal marine (brackish) salinities (MacEachern et al., 2005; Buatois and Mángano, 2011). Reduced rates of deposition are also reflected in more intense biogenic sediment reworking due to an increased colonization window between the successive storm events (MacEachern et al., 2005; Campbell et al., 2016).

7. RESERVOIR IMPLICATIONS

Integration of sedimentological and ichnological datasets allows for the development of a robust depositional model for the Centenario Formation. This paleoenvironmental reconstruction can be used to frame the different sedimentary facies from the perspective of reservoir

characterization. Combination of the facies and petrographic analyses of the cores allowed for a general determination of the most prospective reservoirs within the CHO, SCB, and VAM oilfields. A number of facies represent reservoirs, including F1 (freshwater, ephemeral fluvial channels and crevasse splays), F9 (river-dominated, storm-influenced deltaic distributary channels and mouth bars), F6 (lake/lagoonal deltaic distributary channels), F10 (river-dominated, storm-influenced delta front and proximal prodelta), and rarely F5 (crevasse channel/splay deposits) (Table 4, Figs. 12-13). The reservoir facies have been ranked according to oil saturation values, porosity values (estimated in thin sections), porosity and Klinkenberg-corrected permeability values (derived from laboratory sample analysis), and effective reservoir thickness (determined from core data) (Table 4). Data on the range, mode, median, standard deviation as well as the arithmetic, harmonic, and geometric means have been summarized for the permeability and porosity, these being the most useful parameters for reservoir modeling and flow simulation (Tables 5-6). Porosity in the Centenario reservoirs is of primary and secondary origin (Table 4, Fig. 13). Primary porosity in sandstones is intergranular, and secondary porosity is intragranular (due to partial and total diagenic dissolution of detrital grains, i.e., feldspars and unstable rock fragments). In rocks with a high percentage of carbonate intraclasts, secondary moldic porosity predominates. Diagenetic processes that decrease reservoir porosity include: 1) development of patchy microcrystalline calcite and dolomite cements, pore-occluding kaolinite and illite cements, and patchy poikilotopic anhydrite and gypsum cements; 2) chloritization and sericitization of unstable grains; 3) dolomitization; and 4) syntaxial quartz and feldspar overgrowth (Table 4). Reservoir porosity is enhanced by partial and total grain dissolution, preservation of organic grain envelopes that prevent diagenetic quartz overgrowth , and rare dissolution of dolomite crystals (Table 4). Oil saturation levels have been determined from visual observations (absent, low, medium, and high)

and correlated with well data (i.e., low saturation ~5-10%, medium saturation ~10-40%, and high saturation >40%).

F1 has the best reservoir qualities due to medium-high oil saturation, high porosity (up to 32.7%), permeability (up to 3211 mD), and significant thickness (up to 9.1 m). F1 has been observed within the lower and upper Centenario members and traced within the northeastern part of the study area (CHO and SCB oilfields). Based on facies mapping, the reservoir bodies of F1 are channel forms running in NE-SW and E-W directions (Fig. 12).

F9 is the second-best reservoir with wide areal distribution, medium to low oil saturation levels, substantial porosity (up to 28.8%) and permeability (up to 7364 mD). F9 is present in the lower Centenario member in the central and southwestern parts of the study area (SCB and VAM areas). Effective thickness of the depositional bodies can reach 9.4 m. Based on facies mapping, F9 reservoir bodies constitute channel and bar forms, running predominantly in NE-SW and E-W directions (Fig. 12).

F6 has been ranked lower in regards to its reservoir characteristics due to low to abscent oil saturation and moderate permeability (up to 2016 mD), despite its high porosity (up to 31.6%) and impressive effective thickness (up to 9.0 m). F6 has even less viable reservoir characteristics due to its finer grain size, abundant cements, and highly penetrative diagenetic processes (e.g., calcite, anhydrite, and gypsum cementation; dolomitization; sideritization; alteration of rock fragments and feldspars; quartz overgrowth; etc.). F6 has been identified within the lower Centenario member in the central part of the study area (SCB oilfield). F6 reservoir bodies likely constitute channel and bar forms, stretching in NE-SW and E-W directions (Fig. 12).

F10 has been ranked fourth in its reservoir potential due to its low and commonly patchy oil saturation, explained by lower porosity values (up to 28%) and permeability (up to 895 mD). Its

maximum effective thickness constitutes 3.5 m. F10 has been solely observed within the lower Centenario member (in its lower confines) and is located in the southwestern part of the study area (SCB and VAM oilfields). The interpretation of this facies as delta front suggests that the reservoir stretches in the direction approximately perpendicular to the paleodepositional strike (i.e., SE-NW and S-N) (Fig. 12).

F5 (crevasse splay/channel) has been ranked the lowest amongst the reservoir rocks of the Centenario Formation due to its low oil saturation levels, lower porosity (up to 23.7%), poor permeability (up to 327 mD), and negligible thickness of the depositional bodies (up to 1.8 m). F5 forms a reservoir only within the lower Centenario member in the central part of the study area (SCB oilfield). Channel and wedge forms likely propagate in any possible direction with the tendency of being normal to the NW-SE paleochannel direction (Fig. 12).

Available information from previous reservoir studies within the study area is limited and localized. It has been indicated that within the CHO oilfield, the upper Centenario reservoirs are 6-11 m-thick, include fine- to medium-grained sandstone, and consist primarily of quartz with subordinate amounts of feldspars, lithic fragments, negligible matrix, and calcareous/dolomitic cements (Soraci et al., 2010). Ideal porosity for these sandstones is ~30% and permeability ~1000 mD (Soraci et al., 2010). YPF production data indicate that the lower Centenario member at the VAM oilfield is the main reservoir represented by quartz-feldspathic sandstones with 17% porosity and 80 mD permeability. As such, the current study reaffirmed the previously published reservoir data and provided the necessary paleogeographical framework.

8. CONCLUDING REMARKS

The Lower Cretaceous Centenario Formation has been assessed in detail by combining ichnological and sedimentological core analyses, petrographic, and well-log data. Eleven sedimentary facies and three facies associations have been recognized, providing insights into the paleodepositional environmental settings. The lower Centenario member was deposited in a shallow-marine deltaic environment (i.e., river-dominated, storm-influenced delta), which gradually transitioned into marginal-marine settings by the infill of the accommodation space and progradation. Subsequently, coastal lagoons and sabkhas, ephemeral lakes, and river-dominated lake deltas covered the studied area. Continental sedimentation predominanted during the final stages of the lower Centenario deposition with development of widespread, ephemeral fluvial channel complexes and floodplains, especially towards the east and northeast of the study area. Available data on the upper Centenario member is scarce, and indicates that deposition took place predominantly in continental environments under arid to semi-arid climate conditions. A number of facies have been identified as reservoirs with F1 (freshwater, ephemeral fluvial channels and crevasse splays) representing the best reservoir, and facies F5 (crevasse channel/splay deposits) showing the lowest potential as a reservoir rock.

ACKNOWLEDGMENTS

The authors are grateful to the YPF Neuquén Centenario Group for full cooperation and help in data collection. R. Ruiz is thanked for help in obtaining high-quality microscopic photographs at the Microscopy-Spectroscopy Laboratory, YPF-Tecnología (La Plata). The authors would like to thank reviewers Dr. Andrew La Croix, Dr. Renata Netto, Dr. Lynn Dafoe, and Dr. Nerina Canale for providing insightful comments and suggestions on the initial version of the manuscript.

FUNDING

This research did not receive any specific grant from funding agencies in the public, commercial, or not-for-profit sectors.

REFERENCES

Agirrezabala, L.M., De Gibert, J.M., 2004. Paleodepth and paleoenvironment of *Dactyloidites ottoi* (Geinitz, 1849) from Lower Cretaceous deltaic deposits (Basque-Cantabrian Basin, West Pyrenees). Palaios 19, 276–291.

Arndorfer, D.J., 1973. Discharge patterns in two crevasses of the Mississippi River delta. Marine Geology 15, 269–287.

Beynon, B.M., Pemberton, S.G., Bell, D.D., Logan, C.A., 1988. Environmental implications of ichnofossils from the Lower Cretaceous Grand Rapids Formation, Cold Lake oil sands deposit. In: D.P. James, D.A. Leckie (Eds.), Sequences, Stratigraphy, Sedimentology; Surface and Subsurface. Memoir - Canadian Society of Petroleum Geologists, Calgary, AB, Canada, pp. 275–289.

Bockelie, J.F., 1994. Plant roots in core. In: S.K. Donovan (Ed.), The Palaeobiology of Trace Fossils. John Wiley & Sons, Chichester, UK, pp. 177–199.

Bromley, R.G., 1996. Trace fossils; biology, taphonomy and applications. Chapman & Hall, London, United Kingdom, 361 pp.

Buatois, L.A., Mángano, M.G., 1995. The paleoenvironmental and paleoecological significance of the lacustrine *Mermia* ichnofacies: An archetypical subaqueous nonmarine trace fossil assemblage. Ichnos 4, 151–161.

Buatois, L.A., Mángano, M.G., 1998. Trace fossil analysis of lacustrine facies and basins. Palaeogeography, Palaeoclimatology, Palaeoecology 140, 367–382.

Buatois, L.A., Mángano, M.G., 2002. Trace fossils from Carboniferous floodplain deposits in western Argentina: Implications for ichnofacies models of continental environments. Palaeogeography, Palaeoclimatology, Palaeoecology 183, 71–86.

Buatois, L.A., Mángano, M.G., 2004. Animal-substrate interactions in freshwater environments: Applications of ichnology in facies and sequence stratigraphic analysis of fluvio-lacustrine successions. Geological Society, London, Special Publications 228, 311–333.

Buatois, L.A., Mángano, M.G., 2007. Invertebrate Ichnology of Continental Freshwater Environments. In: W. Miller III (Ed.), Trace Fossils: Concepts, Problems, Prospects, Amsterdam. Elsevier, pp. 285–323.

Buatois, L.A., Mángano, M.G., 2011. Ichnology: Organism-Substrate Interactions in Space and Time. Cambridge University Press, Cambridge, UK, xii + 358 pp.

Buatois, L.A., Delgado, M., Mángano, M.G., 2015. Disappeared almost without a trace: Taphonomic pathways and the recognition of hidden bioturbation events in Eocene storm deposits (Paují Formation, Lake Maracaibo, Venezuela). Annales Societatis Geologorum Poloniae 85, 473–479.

Buatois, L.A., Gingras, M.K., MacEachern, J.A., Mángano, M.G., Zonneveld, J.-P., Pemberton, S.G., Netto, R.G., Martin. A., 2005. Colonization of brackish-water systems through time: Evidence from the trace-fossil record. PALAIOS 20, 321-347.

Cabaleiro, A., 2002. Yacimiento Senal Cerro Bayo. Cuenca Neuquina, YPF, Neuquen, Argentina, pp. 415–420.

Cabaleiro, A., Cazau, L., Lasalle, D., Penna, E., Robles, D., 2002. Los reservorios de la formacion Centenario. Cuenca Neuquina, YPF, Neuquen, Argentina, pp. 407–414.

Cahoon, D.R., White, D.A., Lynch, J.C., 2011. Sediment infilling and wetland formation dynamics in an active crevasse splay of the Mississippi River delta. Geomorphology 131, 57–68.

Campbell, S.G., Botterill, S.E., Gingras, M.K., MacEachern, J.A., 2016. Event sedimentation, deposition

rate, and paleoenvironmental using crowded *Rosselia* assemblages of the Bluesky Formation, Alberta, Canada. Journal of Sedimentary Reseach 86, 380–393.
Casadío, S., Montagna, A.O., 2015. Estratigrafía de la cuenca neuquina. In: Geología de la cuenca Neuquina y sus sistemas petroleros: una mirada integradora desde los afloramientos al subsuelo. Fundación YPF-UNRN, General Roca, Rio Negro, pp. 45–70.
Cevallos, M.F., Rivero, M.T., 2009. Reservoir characterization of unconsolidated coastal plain and littoral sandstones: Case Study of a New Heavy Oil Shallow Play, Neuquina Basin, Western Argentina. Abstracts, Frontiers+Innovation, CSPG, CSEG, CWLS, Calgary, AB, Canada, p. 471.
Cevallos, M.F., Vaamonde, D., Marot, N., Vernon, G., Franco, B., Fortunato, G., 2008. Geological and reservoir characterization of north-eastern Neuquina Basin Heavy Oil Belt, from discovery to EOR in 3 years (Argentina). Abstracts, AAPG Search and Discovery Article #90075, Banff, Alberta, Canada, p. 5.
Cingolani, C., Heredia, S., 2001. Field guide on the Ordovician of the Sierra Pintada, San Rafael Block, Mendoza, 16 pp.
Cohen, A.S., 1982. Paleoenvironments of root casts from the Koobi Formation, Kenya. Journal of Sedimentary Petrology 52, 0401–0414..
Dashtgard, S.E., 2011. Linking invertebrate burrow distributions (neoichnology) to physicochemical stresses on a sandy tidal flat: implications for the rock record. Sedimentology 58, 1303–1325.
Dashtgard, S.E., Gingras, M.K., 2012. Marine invertebrate neoichnology. Developments in sedimentology 64, 273–295.
De Gibert, J.M., Ekdale, A.A., 1999. Trace fossil assemblages reflecting stressed environments in the Middle Jurassic Carmel Seaway of central Utah. Journal of Paleontology 73, 711-720.
de Gibert, J.M., Ekdale, A.A., 2002. Ichnology of a restricted epicontinental sea, Arapien Shale, Middle Jurassic, Utah, USA. Palaeogeography, Palaeoclimatology, Palaeoecology 183, 275-286.
Delpino, D., Santiago, E., Carrizo, N., Méndez, M., Zurita, D., 2014. Miembro Centenario Inferior: un nuevo reservorio en el yacimiento Volcán Auca Mahuida-Risco Alto-Las Manadas. Cuenca Neuquina. Argentina. Abstractos Extendidos, IX Congreso de Exploración y Desarrollo de Hidrocarburos, IAPG, Mendoza, Argentina, p. 65–72.
Diez-Canseco, D., Buatois, L.A., Mángano, M.G., Rodríguez, W.J., Solorzano, E.J., 2015. The ichnology of the fluvial–tidal transition: Interplay of ecologic and evolutionary con- trols. In: P.J. Ashworth, J.L. Best, D.R. Parsons (Eds.), Fluvial-Tidal Sedimentology. Developments in Sedimentology 68, pp. 283–321.
Digregorio, J.H., 1972. Neuquen. In: A.F. Leanza (Ed.), Geologia Regional Argentina. Córdoba, Argentina, Academia Nacional de Ciencias, pp. 439–506.
Dörjes, J., Howard, J.D., 1975. Fluvial-Marine Transition Indicators in an Estuarine Environment, Ogeechee River-Ossabaw Sound. In: G. Hertweck, S. Little-Gadow (Eds.), Senckenbergiana Maritima, v. 7. Estuaries of the Georgia Coast, U.S.A.: Sedimentology and Biology. IV. Senckenbergische Naturforschende Gesellschaft, Frankfurt, Federal Republic of Germany, pp. 137–179.
Frey, R.W., 1990. Trace fossils and hummocky cross-stratification, Upper Cretaceous of Utah. Palaios 5, 203–218.
Frey, R.W., Goldring, R., 1992. Marine event beds and recolonization surfaces as revealed by trace fossil analysis. Geological Magazine 129, 325–335.
Frey, R.W., Pemberton, S.G., Fagerstrom, J.A., 1984. Morphological, ethological, and environmental significance of the ichnogenera *Scoyenia* and *Ancorichnus*. Journal of Paleontology 58, 511–

528.
Fürsich, F.T., Bromley, R.G., 1985. Behavioural interpretation of a rosetted spreite trace fossil: *Dactyloidites ottoi* (Geinitz). Lethaia 18, 199–207.
Gingras M.K., MacEachern J.A., 2012. Tidal Ichnology of Shallow-Water Clastic Settings. In: R. Davis Jr., R. Dalrymple (Eds.), Principles of Tidal Sedimentology. Springer, Dordrecht, pp. 57-77.
Gingras, M.K., MacEachern, J.A., Dashtgard, S.E., 2011. Process ichnology and the elucidation of physico-chemical stress. Sedimentary Geology 237, 115–134.
Gingras, M.K., Pemberton, S.G., Saunders, T.D.A., Clifton, H.E., 1999. The ichnology of modern and Pleistocene brackish-water deposits at Willapa Bay, Washington: variability in estuarine settings. Palaios 14, 352–374.
Gingras, M.K., Dashtgard, S.E., Maceachern, J.A., Pemberton, S.G., 2008. Biology of shallow marine ichnology: a modern perspective. Aquatic Biology 2, 255–268.
Gugliotta, M., Flint, S.S., Hodgson, D.M., Veiga, G.D., 2015. Stratigraphic record of river-dominated crevasse subdeltas with tidal influence. Journal of Sedimentary Research 85, 265–284.
Gunn, S.C., Gingras, M.K., Dalrymple, R.W. and Pemberton, S.G., 2008. Ichnological gradation of subtidal deposits, Ogeechee Estuary, Georgia, USA. In: 2008 AAPG annual convention and exhibition; abstracts volume. Abstracts of annual meeting, American Association of Petroleum Geology.
Hogg, S.L., 1993. Geology and hydrocarbon potential of the Neuquen Basin. Journal of Petroleum Geology 16, 383–396.
Howard, J.D., Frey, R.W., 1973. Characteristic physical and biogenic sedimentary structures in Georgia estuaries. American Association of Petroleum Geologists Bulletin 57, 1169–1184.
Howard, J.D., Frey, R.W., 1975. Regional animal-sediment characteristics of Georgia estuaries. In: G. Hertweck, S. Little-Gadow (Eds.), Senckenbergiana Maritima, v. 7. Estuaries of the Georgia coast, U.S.A.: Sedimentology and Biology. Senckenbergische Naturforschende Gesellschaft, Frankfurt, Federal Republic of Germany, pp. 33–103.
Howell, J.A., Schwarz, E., Spalletti, L.A., Veiga, G.D., 2005. The Neuquen Basin: an overview. In: G.D.Veiga, L.A. Spaletti, J.A. Howell, E. Schwarz (Eds.), The Neuquen Basin, Argentina: A Case Study in Sequence Stratigraphy and Basin Dynamics. Special Publications 252, Geological Society of London, London, UK, pp. 1–14.
Iñigo, J.F.P., Pazos, P.J., Novara, M.E., Comerio, M., 2019. The Lower Cretaceous Centenario Formation: A subsurface unit in the northeastern border of the Neuquén Basin revisited. Journal of South American Earth Sciences 92, 598-608.
Jaglarz, P., Uchman, A., 2010. A hypersaline ichnoassemblage from the Middle Triassic carbonate ramp of the Tatricum domain in the Tatra Mountains, Southern Poland. Palaeogeography, Palaeoclimatology, Palaeoecology 292, 71-81.
Llambías, E.J., Quenardelle, S., Montenegro, T., 2003. The Choiyoi Group from central Argentina: a subalkaline transitional to alkaline association in the craton adjacent to the active margin of the Gondwana continent. Journal of South American Earth Sciences 16, 243–257.
MacEachern, J.A., Pemberton, S.G., 1994. Ichnological aspects of incised- valley fill systems from the Viking Formation of the Western Canada sedimentary basin, Alberta, Canada. In: R.W. Dalrymple, R. Boyd, B.A. Zaitlin (Eds.), Incised-Valley Systems; Origin and Sedimentary Sequences. Society for Sedimentary Geology Special Publication 51, pp. 129–157.
MacEachern, J.A., Gingras, M.K., 2008. Recognition of brackish-water trace fossil suites in the Cretaceous Western Interior Seaway of Alberta, Canada. In: R.G. Bromley, L.A. Buatois, M.G. Mángano, J.F. Genise, R.N. Melchor (Eds.), Sediment-Organism Interactions: A Multifaceted

Ichnology. Society for Sedimentary Geology Special Publication 89, pp. 149–194.
MacEachern, J.A., Bann, K.L., Bhattacharya, J.P., Howell Jr, C.D., 2005. Ichnology of deltas: organism responses to the dynamic interplay of rivers, waves, storms, and tides. In: L. Giosan, J.P. Bhattacharya (Eds.), River Deltas: Concepts, Models, and Examples. Special Publication, 83, Society for Sedimentary Geology, Tulsa, OK, pp. 49–85.
Mángano, M.G., Buatois, L.A., 2004. Reconstructing Early Phanerozoic intertidal ecosys- tems: ichnology of the Cambrian Campanario Formation in northwest Argentina. Fossils Strata 51, 17–38.
Mángano, M.G., Buatois, L.A., Maples, C.G., West, R.R., 1998. Contrasting behavioral and feeding strategies recorded by tidal flat bivalve trace fossils from the Upper Carboniferous of eastern Kansas. Palaios 13, 335-351.
Martinius, A.W., Hegner, J., Kaas, I., Bejarano, C., Mathieu, X., Mjøs, R., 2012. Sedimentology and depositional model for the Early Miocene Oficina Formation in the Petrocedeño Field (Orinoco heavy-oil belt, Venezuela). Marine and Petroleum Geology 35, 354–380.
Melchor, R.N., Genise, J.F., Buatois, L.A.,Umazano, A.M., 2012. Fluvial Environments. In: D. Knaust, R. Bromley (Eds.), Trace Fossils as Indicators of Sedimentary Environments. Developments in Sedimentology 64, pp. 329-378.
Mendiberri, H., 1984. Analisis estratigrafico de la seccion inferior de la Formacion Agrio (incluye Miembro Avile) en el sector norte del Neuquen y sur de Mendoza. Informe interno, YPF, Plaza Huincul, Neuquen, Argentina, 18 pp.
Mercedes-Martin, R., Buatois, L.A. Microbialites and trace fossils from a Middle Triassic restricted carbonate ramp in the Catalan Basin (Spain): evaluating environmental and evolutionary controls in an epicontinental setting. Submitted for publication in Lethaia.
Pemberton, S.G, Wightman, D.M., 1992. Ichnological characteristics of brackish-water deposits: SEPM Core Workshop 17, 141–167.
Pemberton, S.G., MacEachern, J.A., 1997. The ichnological signature of storm deposits: the use of trace fossils in event stratigraphy. In: C.E. Brett, G.C. Baird (Eds.), Paleontological Events. New York, Columbia University Press, p. 73–109.
Pemberton, S.G., Flach, P.D., Mossop, G.D., 1982. Trace fossils from the Athabasca Oil Sands, Alberta, Canada. Science 217, 825–827.
Pollard, J.E., Goldring, R., Buck, S.G., 1993. Ichnofabrics containing *Ophiomorpha*; significance in shallow-water facies interpretation; Organisms and sediments; relationships and applications. Journal of the Geological Society of London 150, 149–164.
Ponce, J.J., Montagna, A.O., Carmona, N.B., 2015. Geología de la Cuenca Neuquina y sus sistemas petroleros: una mirada integradora desde los afloramientos al subsuelo J. J. Ponce, A. O. Montagna, and N. Carmona (eds). Buenos Aires, Argentina, 152 pp.
Rebasa, M., Carbone, O., Cafferatta, A., Meissinger, V., 1992. Analisis sedimentario de la seccion media del M.Inferior de la Formacion Agrio en el area del yacimiento Senal Cerro Bayo (con referencia al engranaje de las Formaciones Centenario/Agrio). Informe interno, YPF, 18 pp.
Reineck, H.E., 1963. Sedimengefuge im Bereich der sudlichen Nordsee. Abhandlungen der Senckenbergischen Natur- forschenden Gesellschaft 505, 1–138.
Retallack, G.J., 2001. Soils of the Past: An introduction to paleopedology. Wiley-Blackwell, Oxford, UK, 420 pp.
Rodríguez, M.W.J., Buatois, L.A., Mángano, M.G., Solórzano,E.J., 2018. Sedimentology, ichnology, and sequence stratigraphy of the Miocene Oficina Formation, Junín and Boyacá areas, Orinoco Oil Belt, Eastern Venezuela Basin. Marine and Petroleum Geology 92, 213-233.

Sato, A.M., Tickyj, H., Llambías, E.J., Sato, K., 2000. The Las Matras tonalitic – trondhjemitic pluton, central Argentina: Grenvillian-age constraints, geochemical characteristics, and regional implications. Journal of South American Earth Sciences 13, 587–610.

Savrda, C.E., Blanton‐Hooks, A.D., Collier, J.W., Drake, R.A., Graves, R.L., Hall, A.G., Nelson, A.I., Slone, J.C., Williams, D.D., Wood, H.A., 2000. *Taenidium* and associated ichnofossils in fluvial deposits, Cretaceous Tuscaloosa Formation, Eastern Alabama, Southeastern U.S.A. Ichnos 3, 227–242.

Schwarz, E., Howell, J.A., 2005. Sedimentary evolution and depositional architecture of a lowstand sequence set: the Lower Cretaceous Mulichinco Formation, Neuquen Basin, Argentina. In: G.D. Veiga, L.A. Spaletti, J.A. Howell, E. Schwarz (Eds.), The Neuquen Basin, Argentina: A Case Study in Sequence Stratigraphy and Basin Dynamics. Special Publication 252, Geological Society of London, London, UK, pp. 109–138.

Schwarz, E., Veiga, G.D., 2007. Caracterizacion facial, paleoambiental y estratigrafico secuencial de la formacion Mulichinco en el yacimiento Volcan Auca Mahuida (Pcia. del Neuquen). Informe para REPSOL-YPF, Desarrollo Área Catriel, Unidad de Negocios Argentina Oeste, Argentina, 97 pp.

Schwarz, E., Veiga, G., Vela, R., Canalis, R., 2008. Paleoambientes y estratigrafia de la Formacion Mulichinco en el yacimiento Volcan Auca Mahuida (cuenca Neuquina, Argentina). Implicancias para la caracterizacion de sellos locales. In: M. Schiuma (Ed.), VII Congreso de Exploracion y Desarollo de Hidrocarburos. Instituto Argentino del Petroleo y del Gas, pp. 1–17.

Scott, J.J., Buatois, L.A., Mángano, M.G., 2012. Lacustrine environments. In: D. Knaust, R.G. Bromley (Eds.), Trace fossils as indicators of sedimentary environments. Elsevier, Amsterdam 64, pp. 379-417.

Shchepetkina, A., Gingras M.K., Pemberton S.G.,MacEachern, J.A., 2016. What does the ichnological content of the middle McMurray Formation tell us? Bulletin of Canadian Petroleum Geology 64, 24-46.

Shchepetkina, A., Gingras, M.K., and Pemberton, S.G., 2016a. Sedimentology and ichnology of the fluvial reach to inner estuary of the Ogeechee River estuary, Georgia, USA. Sedimentary Geology 342, 202–217.

Solórzano, E.J., Buatois, L.A., Rodríguez, M.W.J., Mángano, M.G., 2017. From freshwater to fully marine: Exploring animal-substrate interactions along a salinity gradient (Miocene Oficina Formation of Venezuela). Palaeogeography, Palaeoclimatology, Palaeoecology 482, 30-47.

Soraci, A., García, M.E., Carrizo, N., Propato, J., Rincón, A., 2010. Informe del Modelado Estático. Área de reserva Cerro Hamaca. Informe interno, YPF. Rincon de los Sauces, Neuquen, Argentina, 18 pp.

Spalletti, L.A., Veiga, G.D., 2011. La Formación Agrio (Cretácico Temprano) en la Cuenca Neuquina. In: H.A. Leanza, C. Arregui, O. Carbone, J.C. Danieli, J.M. Vallés (Eds.), Geologia y recursos naturales de la provincia del Neuquen. Relatorio XVIII Congreso Geologico, Imprenta Talleres Trama, Neuquen, Argentina, pp. 145–160.

Taylor, A.M., Goldring, R., 1993. Description and analysis of bioturbation and ichnofabric; organisms and sediments; relationships and applications. Journal of the Geological Society, London 150, 141–148.

Vela, R., Sancho, V., Fasola, M., 2006. Integración de datos geoquímicos en el desarrollo del Yacimiento Volcán Auca Mahuida. Third GQMSP Workshop, Quito, Ecuador.

Vergani, G., Tankard, A.J., Belotti, H.J., Welsink, H.J., 1995. Tectonic evolution and paleogeography of the Neuquen Basin, Argentina. In: A.J. Tankard, R. Suarez Soruco, H.J. Welsink (Eds.), Petroleum Basins of South America. Yacimientos Petrolíferos Fiscales Bolivianos. AAPG Memoirs 62, Academia Nacional de Ciencias de Bolivia, USA, pp. 383–402.

Vottero, A.J., Cafferata, A., 1992. Depositos estuarinos en la mesosecuencia Mendoza Medio (Cretacico Inferior), en el noreste de la cuenca Neuquina. Reporte para YPF, Argentina, 7 pp.

Zonneveld, J.-P., Gingras, M.K., Pemberton, S.G., 2001. Trace fossil assemblages in a Middle Triassic mixed siliciclastic- carbonate marginal marine depositional system, British Columbia. Palaeogeography, Palaeoclimatology, Palaeoecology 166, 249–276.

FIGURE CAPTIONS

Fig. 1. (a) Location of the Neuquén Basin within South America and Argentina. (b) Close-up of (a): the Neuquén Basin (in gray) subdivided into the Andes and Neuquén Embayment regions. It is bounded by the cratonic areas of the Sierra Pintada Massif to the north, the North Patagonian Massif to the south, and the Andean mountains to the west.

Fig. 2. (a) Generalized stratigraphic column of the Neuquén Basin with lithostratigraphy and major tectonic phases (after Howell et al., 2005). (b) Stratigraphic column of the Centenario Formation and its adjacent units within the study area. Generalized lithostratigraphy and a sequence stratigraphic interpretation are provided (after Schwarz and Veiga, 2007).

Fig. 3. Study area. a) Location of the study area (red box) within the Neuquén Basin. b) Close-up of (a): location of the Cerro Hamaca Oeste (CHO), Señal Cerro Bayo (SCB), and Volcan Auca Mahuida (VAM) oilfields.

Fig. 4. A zoomed-in view of SCB showing two cross-sections running from NE to SW along the cored wells. Well distances with the neighbouring oilfields (CHO and VAM) are out of scale, but are shown on the inset map.

Fig. 5. Potential sediment provenance areas for the oilfields in this study (red blocks): the Sierra Pintada Massif borders the Neuquén Basin to the north (Pampa Province) and consists of the plutonic blocks Las Matras and Chadileuvú. The blocks are envisioned to source the clastic material.

Fig. 6. A selected gamma-ray log of the studied interval showing the stratigraphic units and cored sections in the study. The core data cover a small portion of the Centenario Formation. A consistent gamma-ray log kick at the formation top was chosen as a datum.

Fig. 7. Photographs of F1 – F4. (a) Subtle trough cross-stratification in F1. CHO.e-2, depth 590.50 m. (b) Low-angle planar lamination, current-ripple cross-lamination (*rp*), and organic debris preserved along the ripple toesets in F1. CHO.e-4, depth 528.70 m. (c) Bed contact with subangular mudstone rip-up clasts (*rip*), intraclasts (*int*), and abundant phytodetrital material (*od*) in F1. SCB-27, depth 1596.50 m. (d) Massive silty mudstone with soft-sediment deformation structures (*ssd*) and siderite concretions (*cn*) in reddish siltstone of F2. CHO.e-2, depth 581.20 m. (e) Silty mudstone of F2 with a siderite concretion (*cn*). CHO.e-4, depth 517.30 m. (f) Sandstone of F3 with rhizoliths (*rz*) and yellowish diagenetic staining. (g) Thinly laminated siltstone and mudstone of F3, with mottling by rhizoliths (*rz*). SCB-102, depth 1393.40 m. (h) Mudstone and sideritized siltstone of F4, with planar parallel lamination (*pl*), climbing ripples (*clm*), and lenticular bedding (*len*). A large dike (*dy*) cross-cuts the primary sedimentary fabric. SCB-9, depth 1569.55 m. (i) Sheet-like microbialites (*mcr*) in F4. SCB-27, depth 1565.20 m. (j) Muddy sandstone of F4 with climbing current-ripple cross-lamination (*clm*) and *Taenidium* (*Ta*). SCB-9, depth 1601.60 m. (k) Locally, F4 consists of sandstone interbeds with spotty calcite (*Ca*) and anhydrite/gypsum (*An*) cements. Current ripples (*rp*) and cracks filled with organic residue (*cr*) are also present. SCB-9, depth 1598.30 m.

Fig. 8. Photographs of F5 – F8. (a) Climbing (*clm*) and wave/combined-flow ripples (*rp*) covered by mudstone drapes (*md*) in F5. A few *Planolites* (*Pl*) and a single sand dike (*dy*) are visible. SCB-9, depth 1571.70 m. (b) Interbedded sandstone and siltstone with thin organic detritus draping laminae (*od*) of F5. Sediments are reworked by a low-diversity suite of ?*Arenicolites* (*Ar*?), *Planolites* (*Pl*), and *Paleophycus* (*Pa*). Combined-flow ripples (*rp*) are locally visible in sandstone. SCB-27, depth 1598.30 m. (c) Organic drapes (*od*) in F5 are locally cross-cut by ?*Taenidium* (*Ta*) and *Planolites* (*Pl*). Climbing (*clm*) and combined-flow ripples (*rp*) form characteristic wavy bedding. SCB-27, depth 1599.10 m. (d) Mottled sediment appearance of F6 with wavy lamination (*wv*) due to uneven anhydrite/gypsum (*An*) cementation. SCB-102, depth 1381.55 m. (e) Oil-saturated sandstone of F6 with organic detritus draping laminae (*od*) and a lag of mudstone and coal rip-up clasts (*rip*). SCB-102, depth 1387.00 m. (f) Abundance of organic material (*od*) and coalified clasts (*co*) in F6. SCB-102, depth 1395.90 m. (g) Monospecific trace-fossil suite of *Taenidium* (*Ta*) in F7. Desiccated mudstone is broken into mudstone rip-up clasts (*rip*). SCB-27, depth 1545.40 m. (h) Floating sand grains (*flt*) in a soupy mud of F7, a lag of mudstone rip-up clasts (*rip*), and soft-sediment deformation structures (*ssd*). SCB-27, depth 1561.80 m. (i) Good preservation of primary sedimentary structures in F7: planar parallel lamination (*pl*) and current ripples (*rp*). The fabric is penetrated by possible rhizoliths (*rz*?). Biogenic mottling is notable in some layers (*mt*). SCB-102, depth 1385.00 m. (j) Microbial mats (*mi*) of F8 with wavy appearance, scattered bioclasts (*bio*), *Arenicolites (Ar*), and calcium-filled cracks (*cr*). Calcium (*Ca*) and anhydrite/gypsum (*An*) cements are present. SCB-11, depth 1631.70 m. (k) Microbial mats (*mi*) of F8 forming undulatory (wavy) and wrinkled laminae. Biogenic mottling (*mt*) is visible in the upper part of the sample. Calcium (*Ca*) and siderite (*Sid*) cements are spotted. SCB-10, depth 1613.90 m.

Fig. 9. Photographs of F9 – F11. (a) Low-angle to parallel laminated, oil-saturated sandstone of F9 with organic debris (*od*) along the depositional surfaces and a cryptic bioturbation (*cry*). VAM-80, depth 2615.55 m. (b) Ripples in F9 are marked by organic debris (*od*) with abundant bioturbation by *Haentzschelinia* (*Ha*). VAM-80, depth 2618.20 m. (c) Sets with high-angle planar stratification in F9 separated by a reactivation surface (*rct*). Mudstone rip-up clasts (*rip*) appear above the reactivation surface. Lower part of the illustrated interval is cryptically bioturbated (*cry*). VAM-80, depth 2679.60 m. (d) Intergradation of calcite-cemented sandstone (*Ca*) with bioclasts (*bio*) and intraclasts (*int*) into grainstone with intraclasts (*int*) in F9. Extensive moldic porosity (*mol*) formed within the bioclasts. SCB-10, depth 1643.80 m. (e) Lam-scram fabric, where the laminated (L) interval is represented by hummocky cross-stratification (*HCS*) marked by organic debris (*od*) and fugichnia (*esc*), whereas the scrambled (S) intervals are thoroughly bioturbated by *Ophiomorpha* (*Op*) and *Haentzschelinia* (*Ha*). SCB-8, 1695.30 m. (f) Interval with soft-sediment deformation structures (*ssd*) is overlain by a cryptically bioturbated interval (*cry*) with low-angle planar lamination in F10. VAM-80, depth 2680.50 m. (g) Predominance of primary sedimentary structures in F10: hummocky (*HCS*), swaley cross-stratification (*SCS*), and planar parallel lamination (*pl*). Organic debris (*od*) marks the depositional surfaces. Cryptic bioturbation (*cry*) and fugichnia (*esc*) are locally present. SCB-8, depth 1694.40 m. (h) Abundant organic debris (*od*), planar parallel lamination (*pl*), and extensive sediment reworking by cryptobioturbation (*cry*) in F10. SCB-10, depth 1647.10 m. (i) Intensely bioturbated sandstone in F10 containing small specimens of *Ophiomorpha* (*Op*). Partial oil saturation. SCB-10, depth 1632.80 m. (j) Thoroughly bioturbated sandstone in F11 containing *Asterosoma* (*As*) overprinted to biogenic mottling (*mt*). Underlying heterolithic interval displays *Rhizocorallium* (*Rh*), a thin HCS sandstone layer and mudstone interbeds (*fld*). SCB-8, depth 1697.30 m.

Fig. 10. Cross-section 1 (for location refer to Fig. 4) summarizes vertical facies distribution and spatial facies associations distribution based on the core (FA1-FA3) and well-log data (FA1-FA3) analyses. MD refers to measured depth, SP - to spontaneous potential, and GR – to gamma ray. Color fill in the GR log indicates likely rock lithology, ranging from sandstone (yellow color) to mudstone (dark brown color).

Fig. 11. Cross-section 2 (for location refer to Fig. 4) summarizing vertical facies distribution and spatial facies associations distribution based on the core (FA1-FA3) and well-log data (FA1-FA3). Two lithologs from well VAM-80 provide details on the facies characteristics and facies stacking patterns. MD refers to measured depth, SP - to spontaneous potential, and GR – to gamma ray. Color fill in the GR log indicates likely rock lithology, ranging from sandstone (yellow color) to mudstone (dark brown color).

Fig. 12. Illustration of a proposed paleodepositional model for the Centenario Formation within the study area.

Fig. 13. Petrographic expression of the Centenario reservoirs. PPL stands for transmitted, plain-polarized light. (a-c) Microphotographs of F1: a) 2.5x PPL. Low-magnification image of a moderately to poorly sorted, medium-grained, feldspathic litharenite with kaolinite rims and patchy distribution of dolomite crystals. Excellent intergranular porosity (~24-28%). CHO.e-2, depth 584.59 m. b) 10x PPL. High-magnification image of a porous layer within a poorly sorted fine-grained, feldspathic litharenite with a rounded, high relief ?monazite grain (center). Excellent

intergranular porosity (~20%). CHO.e-4, depth 521.48 m. c) 10x PPL. High-magnification image of a well sorted, medium-grained, feldspathic litharenite with an altered shale intraclast (center). Good to very good intergranular and intragranular (along the cleavage planes) porosity (~15%). SCB-59, depth 1525.13 m. (d-f) Microphotographs of F9: d) 10x PPL. High-magnification image of a moderately sorted, feldspathic litharenite with volcanic (center) and metamorphic (upper right corner) rock fragments. Moderate intergranular and intragranular porosity (~5-7%). VAM-80, depth 2614.20 m. e) 10x PPL. High-magnification image showing a moderately sorted, medium-grained, feldspathic litharenite with accessory grains of tourmaline (yellow and dark-green). Good intergranular and intragranular porosity (~10-12%). VAM-80, depth 2610.22 m. f) 5x PPL. High-magnification image of a moderately sorted, medium-grained feldspathic litharenite with patchy ?dolomite and macrocrystalline siderite (yellow arrows) cements. Good intergranular and more rarely intragranular porosity (~10-12%). VAM-80, depth 2610.22 m. (g-i) Microphotographs of F6: g) 2.5x PPL. Low-magnification image of a poorly sorted, fine- to medium-grained, feldspathic litharenite with cemented and porous patches. Moderate to good intergranular porosity (~7-12%). SCB-102, depth 1380.47 m. h) 10x PPL. High-magnification image of a very fine- to fine-grained, feldspathic litharenite with fragments of organic material with cellular structure (wood/leaf). Very poor fracture and intergranular porosity (~1%). SCB-102, depth 1396.0 m. i) 10x PPL. High-magnification image of a bimodal, very fine- to medium-grained, feldspathic litharenite with poikilotopic calcite cement. Poor intergranular porosity (~1-2%). SCB-102, depth 1381.26 m. (j-k) Microphotographs of F10: j) 2.5x PPL. Low-magnification image of a well sorted, very fine-grained, lithic arkose. Poor intergranular porosity (~2-4%). VAM-80, depth 2678. 95 m. k) 2.5x PPL. Low-magnification image of a fine- to medium-grained, feldspathic litharenite with a tourmaline grain (black arrow) and patchy calcite cement. Poor

intergranular porosity (~1-2%). SCB-10, depth 1622.23 m. (l) Microphotograph of F5. 5x PPL. High-magnification image of a moderately sorted, fine-grained, feldspathic litharenite with argillaceous matrix and patchy microcrystalline calcite cement. Moderate intergranular porosity (~5-7%). SCB-10, depth 1576.53 m.

Table 1. Previous paleoenvironmental interpretations of the Centenario Formation.

Table 2. Sedimentary facies and facies interpretations of the Centenario Formation. For grain size, L – signifies lower, and U – means upper.

Table 3. Summary table depicting the constituent facies of FA1-FA3 with the interpreted subenvironments.

Table 4. Summary table with the most prospective reservoirs for the Centenario Formation within the study area.

Table 5. Summary table showing statistical reservoir permeability data, where K gas is the laboratory measured gas permeability, and K klik is the Klinkenberg-corrected permeability value.

Table 6. Summary table showing statistical reservoir porosity data.

Lower Centenario Formation	Upper Centenario Formation	Source
Variety of marginal-marine environments		Cabaleiro, 2002
Littoral zone with moderate wave action (e.g., littoral bars, beaches, tidal flats, and tidal channels)		Mendiberri, 1984
Platform (e.g., storm-reworked bars, shoreface, and offshore), lagoon (cap rocks), and estuarine channels (reservoir rocks)	N/A	Rebasa et al., 1992
Platform, tidal flats, estuarine channels, and lagoon	N/A	Vottero and Cafferata, 1992
Coastal-plain to shallow-marine environments (e.g., ebb-tidal deltas, tidal channels, and barrier islands)	N/A	Cevallos et al., 2008 Cevallos and Rivero, 2009
Distal fluvial channels, estuaries, and tidal flats	Shallow-marine environments to fluvial channels	Soraci et el., 2010
Littoral, deltaic, and fluvial environments	Fluvial environments	Casadío and Montagna, 2015; Ponce et al., 2015
Restricted bay, marginal-marine, tidal flat with minor wave reworking, tide-dominated delta	Shoreface, wave-dominated delta, embayment, estuary, paralic, fluvial	Iñigo et al., 2019

Facies association	Facies	Sedimentology	Ichnology	Interpretation	Distribution
FA1: Continental (fluvial) environment	F1: Trough cross-stratified, fine- to medium-grained sandstone	Poorly to moderately sorted, trough cross-stratified, massive, planar parallel and low- to high-angle laminated, fine- (L) to medium- (L) grained sandstone with some grain-size striping. Mica, medium-sized sand grains, and organic debris preserved along the foresets. Current and climbing ripples marked by organic debris. Rare mudstone clasts and soft-sediment deformation structures. Erosive bed contacts marked by mudstone rip-up clasts, intraclasts, and sand grains. Sporadically distributed spots of secondary cements (e.g., calcite, anhydrite/gypsum). Individual beds 0.3-2.0 m thick (average 1 m), forming 0.45-9.1 m thick intervals (average 2.2 m). Generally sharp basal contacts. Low to heavy oil saturation.	Mostly barren of trace fossils (BI 0) with only rare occurrences of *Skolithos* in discrete layers (BI 0-1).	Freshwater fluvial channels and crevasse splays of ephemeral to perennial nature based on predominantly medium sandstone grain size, high-energy unidirectional sedimentary structures (i.e., trough cross-stratification, low- to high-angle planar lamination), paucity of trace fossils, abundant organic detritus, and considerable thickness (up to 9.1 m). Calcite cement caused by early diagenetic processes. Spotty anhydrite/ gypsum cements indicate arid and highly evaporitic settings. In wells SCB-9, SCB-27, and SCB-59, F1 is interpreted as deposits of low-gradient fluvial system and of hyperpycnal flows in a lake environment based on thinner bodies (0.5-2.5 m), intercalation with mudstone and siltstone with dikes and microbialites, evidence of microbial action, soft-sediment deformation, starved and climbing current ripples.	Wells CHO.e-2, CHO.e-4, SCB-9 SCB-27, and SCB-59
	F2: Muddy heterolithics with starved current ripples	Interlaminated greenish muddy siltstone, argillaceous fine- (U) to medium- (L) grained sandstone, and greenish-gray mudstone with planar parallel lamination, lenticular bedding, starved current ripples, soft-sediment deformation structures, microfaults, and mudstone rip-up clasts. Floating medium-sized sand grains, oxidized and sideritized intraclasts, pyrite nodules, and local calcite and dolomite cements. Very thin laminations of possibly microbial origin. Beds 0.2-1 m thick (average 0.5 m), forming 0.4-5.2 m thick intervals (average 1.3 m). Generally sharp basal contacts. Absent to low (in sandy lamina) oil saturation.	No trace fossils (BI 0)	Abandoned ephemeral fluvial channels, crevasses, and floodplains. Overall fine-grained deposits indicate predominantly low-energy conditions (i.e., thin planar parallel lamination, lenticular bedding, starved current ripples) with intermittent pulses of high energy manifested in silty and sandy beds, floating medium- (U) sized sand grains, and other intraclasts. Abundance of soft-sediment deformation features and syndepositional microfaults points to the water-saturated nature of the substrate and presence of inclined depositional surfaces. Oxidized and sideritized intraclasts indicate highly oxidizing environmental conditions with extended subaerial exposure between the depositional events. Incipient calcite and dolomite cementation suggest arid, desert-like climate.	Wells CHO.e-2 and CHO.e-4
	F3: Thinly laminated siltstone with rhizoliths	Siltstone to very fine-grained sandstone with mottled appearance. Color diagenetically changed (CHO.e-2, SCB-59), some visible original bedding, and partial lithification with calcite cement. In SCB-102, thinly interlaminated siltstone and mudstone. Beds 0.1-0.3 m thick (average 0.15 m), forming 0.1-0.5 m thick intervals (average 0.3 m). Generally gradational basal contacts. Absent oil saturation.	Abundant rootlets (BI 2-4)	Immature paleosols (some developed in interfluve areas). Two types of paleosols: 1) sandy paleosols represented by fine- to medium-grained sandstone with a few rhizoliths, and 2) interlaminated siltstone and mudstone with abundant vertical rootlets. Negligible thickness of F3 due to partial or total removal by migrating channels. Calcite/ dolomite cement due to quick calcification as calcite actively percolates in the desert soil profile. Penetrative and relatively straight tap roots indicate well-drained paleosols with low water table and sporadic water availability.	Wells CHO.e-2, SCB-59, and SCB-102

FA2: Continental to marginal-marine environment	F4: Muddy heterolithics with dikes and microbialites	Interlaminated dark gray and green mudstone and brownish-red siltstone with abundant oscillating and climbing current ripples, lenticular and planar parallel lamination, syneresis cracks, soft-sediment deformation structures, syndepositional microfaults, sand- and mud-filled dikes and cracks, and microbialites (domes and sheet-like). Less common mudstone clasts, stylolites, breccia, calcite-filled thin cracks, floating sand grains, and shell debris. Spotty, pore-occluding calcite, dolomite, siderite, anhydrite, and gypsum cements. Local mottling. Individual beds 0.05-0.9 m thick (average 0.45 m), forming 0.1-2.3 m thick intervals (average 0.8 m). Gradational to sharp basal contacts. No oil saturation.	Low-moderate ichnodiversity; sporadic distribution; sparse to moderate bioturbation (BI 0-3). *Skolithos, Arenicolites, Palaeophycus, Planolites, Taenidium,* probable rhizoliths. Trace fossils predominantly in fine-grained fraction.	Shallow-water ephemeral lakes and their margins (mudflats) with little vegetation based on fine-grained deposits with low-energy sedimentary structures (e.g., lenticular and planar parallel lamination) interbedded with higher-energy sedimentary structures (e.g., oscillating and climbing current ripples, mudstone clasts, floating coarse sand grains, and shell debris). Presence of evaporites, including dolomite cement, indicates increase in lake evaporation rate during hot seasons in arid to semi-arid climate conditions. Microbialites point out to drops in the lake water level. Microbial laminites, solution collapse breccias, and ?root traces suggest frequent wetting and drying in the ephemeral lake (hints to strong seasonality). Abundant soft-sediment deformation structures, syndepositional microfaults, dikes and cracks - periods with widespread water-saturated substrates and possible triggers, i.e. rapid sediment loading caused by hyperpycnal lake underflows, storm wave action or seismic shocks.	Wells SCB-9, SCB-27, and SCB-59
	F5: Very fine- to fine-grained sandstone with climbing and combined-flow ripples	Gray, wavy and low-angle planar laminated, very fine- (L) to fine- (U) grained sandstone with climbing current and combined-flow ripple cross-lamination, mudstone and organic drapes, mudstone rip-up clasts, sand- and mud-filled dikes, and rare syneresis cracks. Sandstone interbedded with lenticular bedded mudstone with starved climbing ripples. Several reactivation surfaces. Common calcite cementation. Individual beds 0.1-0.3 m thick (average 0.2 m), forming 0.15-1.8 m thick intervals (average 0.6 m). Sharp to erosional basal contacts. Low to absent oil saturation.	Low ichnodiversity; sporadic distribution; low intensity of bioturbation (BI 0-1). *Skolithos, Arenicolites, Palaeophycus, Planolites, ?Taenidium,* fugichnia, rhizoliths.	Crevasse channel/splay deposition within upper delta plain and ephemeral lake environments based on negligible thickness of deposits, sharp bases, fine-grained sandstone lithology, predominant fining-upward grain-size trend, and intimate association with the mudflat and interdistributary bay facies (F4, F7). Mudstone clast breccia - high initial hydraulic energy with the sediment-laden flow breaching through the channel levee and dissipating onto the mudflat of the ephemeral lake or interdistributary bay. Wavy and low-angle planar laminations form at initial waning stages; climbing current ripples – at final waning stages associated with rapid flow-velocity deceleration and ripple aggradation. Single or multi-storey events with occasional preservation of reactivation surfaces.	Wells SCB-9, SCB-10, SCB-27, SCB-52, SCB-59, and SCB-102
	F6: Medium- to fine-grained sandstone with planar parallel and wavy lamination	Light brown to light gray, wavy, low-angle and planar parallel laminated, and trough cross-stratified, fine- (L) to medium- (U) grained sandstone with soft-sediment deformation structures, current and climbing ripple cross-lamination, abundant organic debris, grain-size striping, mudstone rip-up clasts, and organic drapes. Common rip-up clast lags at the base or above reactivation surfaces. Predominant coarsening-upward trend. No trend or a fining-upward trend can	Low ichnodiversity; sporadic distribution; low intensity of bioturbation (BI 0-1). *Palaeophycus, Lockeia,* cryptic. Trace fossils mainly in the coarse-grained portion.	Terminal distributary channels and mouth bars of a river-dominated delta formed in a lake and lagoon environment. Deltaic interpretation supported by a coarser-grained sediment fraction, trough cross-bedding, abundance of continentally derived organic matter, flow-waning structures, and cycles of activity marked by erosional bases. Soft-sediment deformation structures - variations in the rate of sediment loading during periods of high freshwater discharge. Current and climbing ripples suggest periodic shallowing of the flow. Stacking of successions indicates rapid channel bifurcation and avulsion: common in	Wells SCB-10, SCB-27, SCB-51, SCB-59, and SCB-102

		be present. Common patchy calcite, dolomite, anhydrite, and gypsum cements. Beds 0.3-1.3 m thick (averages 1 m), forming 0.3-9.0 m thick intervals (averages 2.8 m). Sharp to erosional basal contacts. Medium to absent oil saturation.		dynamic, river-dominated deltas. Shallow-water conditions of the receiving body deduced by diminished thickness of F6 packages indicating reduced accommodation space.	
	F7: Mudstone with lenticular bedding	Dark gray shale/mudstone with red-colored siltstone and sandstone lenses, mudstone rip-up clasts, abundant soft-sediment deformation structures, syndepositional microfaults, dikes, cracks, floating bioclasts and sand grains, intact and brecciated microbialites, ?syneresis cracks, massive, planar parallel and wavy lamination, lenticular bedding, current ripple and climbing ripple cross-lamination, and organic debris. Common biogenic mottling. Zones with calcite and siderite cements. Individual beds 0.1-0.8 m thick (average 0.3 m), forming 0.1-3.6 m thick intervals (average 0.9 m). Sharp to erosional basal contacts. No oil saturation.	Low ichnodiversity; sporadic distribution; variable intensity of bioturbation (BI 0-4, predominant BI 2-4). *Skolithos, Arenicolites, Diplocraterion, Palaeophycus, Planolites, Taenidium,* possible rhizoliths.	Shallow-water bays and mudflats of the delta plain. Fine-grained deposits, low-energy sedimentary structures (e.g., planar parallel, wavy and lenticular bedding) interbedded with higher-energy sedimentary structures (e.g., ripple cross-lamination, rip-up clasts, and soft-sediment deformation structures) indicate a generally stable, low-energy depositional environment dominated by deposition from suspension with minor traction currents. Muddier areas – deposition at central bay and surrounding muddy flats; silty and sandy heterolithic deposits - areas with more pronounced sand influx. Abundant soft-sediment deformation structures, syndepositional microfaults, and dikes indicate periods with widespread water-saturated substrates and rapid sediment loading. Brecciated intervals - disruption of semi-cohesive to cohesive sediments without significant sediment transport. Microbial laminites, solution collapse breccias, and ?root traces show frequent wetting and drying (hints to seasonality).	Wells SCB-10, SCB-27, SCB-51, SCB-52, SCB-102, and VAM-80
	F8: Siltstone and sandstone with anhydrite, calcite, and dolomite cements	Very thinly laminated, anhydrite/gypsum-cemented, calcareous to dolomitic siltstone, sandstone, and mudstone. Sedimentary structures include microbial/algal wrinkled lamination, wavy, lenticular bedding, oscillatory ripple cross-lamination, scattered bioclastic debris, syneresis cracks, soft-sediment deformation structures, dikes, mudstone rip-up clasts, organic debris, calcium-filled cracks, and stylolites. Some biogenic mottling. Individual beds 0.05-0.3 m thick (average 0.15 m), forming 0.4-1.6 m thick intervals (average 1.1 m). Sharp to slightly erosional basal contacts. No oil saturation.	Low ichnodiversity; sporadic distribution; variable intensity of bioturbation (BI 0-4). *Skolithos, Palaeophycus, Planolites, Teichichnus.*	Shallow coastal lagoon or sabkha. Abundant evaporitic cements develop in supratidal settings of arid climates. Undulatory and wrinkled thin laminae represent intermittent growth of algal/microbial bodies or salt-crust growth and dissolution acting in low-relief areas of sabkhas. Microbial mats are especially common in protected intertidal to supratidal environments of shallow lagoons and sabkhas. Syneresis cracks - periods of freshwater introduction into the depositional setting. Mudstone rip-up clasts and scattered bioclastic debris likely represent deposition during washover events. Wavy, lenticular bedding, and oscillatory ripple cross-lamination - a generally quiescent depositional setting punctuated by short intervals of traction deposition (possibly by wave action).	Wells SCB-10 and SCB-11
FA3: Shallow-marine (deltaic) environment	F9: Very fine- to medium-grained sandstone with planar	Gray to brown, massive, trough cross-stratified, wavy and planar parallel laminated, very fine- (U) to medium- (L) grained sandstone with climbing ripples, soft-sediment deformation structures,	Low ichnodiversity; sporadic distribution; variable intensity of bioturbation (BI 2-	River-dominated, storm-influenced delta with distributary channels, terminal distributary channels, and mouth bars based on prevailing unidirectional sedimentary structures (e.g., planar parallel, low- and high-angle planar lamination, trough cross-stratification, climbing ripple cross-	Wells SCB-8, SCB-10, SCB-11, SCB-52, and VAM-80

	parallel and trough cross-stratification	syndepositional microfaults, mudstone/organic drapes, intraclasts, mudstone rip-up clasts, organic debris, mudstone layers, scattered granules, intraclasts, and bioclasts. Some layers with abundant bioclasts and intraclasts show moldic porosity. Calcareous, dolomitic, anhydrite, and gypsum cements locally present. Erosional and reactivation surfaces in stacked packages with a predominantly coarsening-upward pattern. Rare biogenic mottling. Beds 0.25-2.1 m thick (average 1 m), forming 0.25-9.4 m thick intervals (average 2.1 m). Gradational to sharp and, rarely, erosional basal contacts. Low to medium oil saturation.	6). *Skolithos, Arenicolites, Ophiomorpha, Palaeophycus, Planolites, ?Teichichnus, Thalassinoides, Haentzschelinia,* fugichnia, local cryptic bioturbation.	lamination), reworking by waves (e.g., wavy lamination) and possibly tides (mudstone/organic drapes), abundant plant debris, mudstone clasts, and a typical coarsening-upward pattern. Thin depositional bodies (1-3 m) – a reduced accommodation space (i.e., a ramp setting), where river-dominated deltas debouche into a shallow basin and form multiple distributary channels. River dominance based on coarse sediment size (including granules, intraclasts, and bioclasts), presence of fluid mud layers, and variably scaled soft-sediment deformation features. Fluid mud layers caused by hypo- and hyperpycnal flows as phyto-detrital pulses. Soft-sediment deformation structures formed due to high sedimentation rates and sediment overloading. Storm influence inferred based on the exceptional sandstone cleanliness.	
	F10: Siltstone to fine-grained sandstone with soft-sediment deformation structures	Light- to dark-gray, low- to high-angle planar laminated, hummocky (HCS) and swaley (SCS) cross-stratified, laminated to scrambled ("lam-scram") siltstone to fine- (U) grained sandstone with abundant soft-sediment deformation structures, syneresis cracks, oscillation ripples, and intraclasts. Some intervals contain calcite/dolomite cement and floating bioclasts. Local biogenic mottling. Individual beds 0.15-1 m thick (average 0.4 m), forming 0.3-3.5 m thick intervals (average 1.3 m). Gradiational to sharp basal contacts. Negligible oil saturation.	3 ichofossil suites. Laminated (BI 0-2) and scrambled intervals (BI 3-6). Fugichnia, cryptic, *Ophiomorpha*, *Palaeophycus*, *Skolithos,Diplocraterion, Haentzschelinia Lockeia*, *Bergaueria, Thalassinoides, Planolites*, *Teichichnus.*	River-dominated, storm-influenced delta front. River dominance due to finer sediment size, abundant soft-sediment deformation structures, organic detritus, and syneresis cracks. Soft-sediment deformation structures imply sediment overloading, dewatering, and liquefaction – proximity to delta front. Organic material represents phytodetrital pulses common in river-dominated deltas during peak-flood discharge. Syneresis cracks - salinity fluctuations (i.e., freshets). Higher-energy sedimentary structures (i.e., laminated) - increased wave activity, i.e. storm erosion and tempestite deposition.	Wells SCB-8, SCB-10, and VAM-80
	F11: Interbedded mudstone and very fine-grained sandstone with HCS	Structureless, lenticular-bedded mudstone interbedded with planar parallel laminated, low- to high-angle cross-stratified, massive and wavy bedded, very fine-grained sandstone with organic debris, mudstone rip-up clasts, bioclasts, and reactivation surfaces. Common soft-sediment deformations. Individual beds 0.03-0.25 m thick (average 0.13 m), forming 0.2-3.0 m thick intervals (average 0.7 m). Sharp basal contacts. Absent to low oil saturation.	Moderate to high ichnodiversity; highly variable intensity (BI 0-6). Cryptic, *Lockeia, Ophiomorpha, Thalassinoides, Palaeophycus, Planolites*, *Teichichnus, Haentzschelinia, Asterosoma, Rhizocorallium, Phycosiphon, Chondrites.*	River-dominated, storm-influenced prodelta. Storm influence evidenced by high-energy sedimentary structures (i.e., planar parallel lamination, low- and high-angle cross-stratification, HCS, wavy bedding, ripple cross-lamination, and reactivation surfaces). Finer grain size and absence of SCS - slower, continuous rates of deposition in a more distal setting.	Wells SCB-8, SCB-10, and VAM-80

HIGHLIGHTS

- The Centenario Formation is a significant producer of oil and gas in the Neuquén Basin, Argentina
- Detailed sedimentological, ichnological, petrographical, and petrophysical analyses provided insight into the paleodepositional environments
- The Centenario Formation was deposited in a river-dominated, storm-influenced deltaic environment, which gradually transitioned into the marginal-marine (e.g., coastal lagoons, sabkhas, ephemeral lakes) and continental depositional settings (e.g., ephemeral fluvial channels, crevasse splays, abandoned channels, floodplains, and paleosols)

Declaration of interests

☐ x The authors declare that they have no known competing financial interests or personal relationships that could have appeared to influence the work reported in this paper.

☐The authors declare the following financial interests/personal relationships which may be considered as potential competing interests:

Dr. Alina Shchepetkina